AIAA JOURNAL
Vol. 42, No. 2, February 2004

Comparison of Two Waveguide Methods for Educing Liner Impedance in Grazing Flow

M. G. Jones,* W. R. Watson,† M. B. Tracy,‡ and T. L. Parrott§
NASA Langley Research Center, Hampton, Virginia 23681-2199

Acoustic measurements taken with several liners in a flow impedance tube are used to assess two waveguide methods, the single mode method (SMM) and the finite element method (FEM), for impedance eduction in the presence of uniform grazing flow. Both methods use complex acoustic pressure data acquired over the liner length to educe the liner impedance. The SMM is based on the assumption that the sound pressure level and phase decay rates of a single progressive mode can be extracted from the measured complex acoustic pressures. No a priori assumptions are made in the FEM regarding the measured data. For no-flow conditions, the accuracy of each method is demonstrated by the excellent agreement between no-flow impedances educed in a grazing incidence tube and those acquired in a normal incidence tube. For grazing flow conditions (Mach numbers up to 0.5), the relative accuracy of the two waveguide methods is demonstrated by comparing the impedances educed with the FEM to the corresponding results for the SMM. Significant discrepancies occur for both methods for tests conducted at 0.5 kHz. Possible explanations for these discrepancies are explored with, as yet, no clear answer. Above 0.5 kHz, the results indicate the SMM can be used when the acoustic pressure profile is dominated by a single progressive mode, whereas the FEM can be used for all cases.

Nomenclature

c, ρ	=	sound speed and ambient density in duct
d, r_{eq}	=	equivalent depth and radius of liner channel
d_s, l_s	=	depth and length of ceramic tubular liner segment
f, ω, t	=	frequency, angular frequency ($= 2\pi f$) and time
H, L	=	height and length of duct
i	=	unit imaginary number ($= \sqrt{-1}$)
k, k_x, k_y	=	wavenumbers (free space, axial and transverse)
L_1, L_2	=	location of leading and trailing edges of liner
M	=	Mach number, averaged over duct cross section
N	=	number of points used in statistical calculations
p, p_{ref}, p_s	=	general, reference ($= 20\ \mu$Pa) and source-plane acoustic pressures
S_j, S	=	individual segment and total surface areas
SPL, ϕ	=	sound pressure level and phase angle
x, y, z	=	axial, vertical, and transverse coordinates
x_j	=	wall measurement location
β_j, β_u	=	individual segment and effective uniform admittances
ζ, ζ_u, ζ_{exit}	=	dimensionless wall, effective uniform, and exit-plane impedances (normalized by ρc)
θ, χ	=	dimensionless impedance components: resistance and reactance $\zeta = \theta + i\chi$
μ, σ	=	error mean and standard deviation

Subscripts

FEM, SMM	=	result achieved using the finite element and single mode methods
$M = 0.1$	=	result achieved at $M = 0.1$ (similar for $M = 0.3$ and 0.5)
NIT	=	result measured in normal incidence tube

Introduction¶

THE continual improvement of acoustic liner design, with special emphasis on efficiency and bandwidth, is critical to commercial aircraft noise emission control. To that end, it is becoming increasingly important to achieve the optimum liner impedance for each portion of the engine nacelle. To achieve this goal, measurement and analysis methods must be further developed to educe more accurately the normal incidence acoustic impedance of test liners in the presence of grazing flow. This continued development is critical to the improvement of existing impedance prediction tools, such that the acoustic behavior of various liners can be predicted with confidence without the need for costly duct liner tests.

Typically, either in situ[1–3] or waveguide[4–10] methods are used to educe the acoustic impedance of test liners. Of the waveguide methods, much effort has been placed on creating conditions where simple modal approaches[4–8] can be applied that typically do not require significant computational capability. One of the earlier examples of this was the "T-tube" method,[4] in which a normal incidence tube is mounted onto the side wall of a grazing incidence flow tube. The sample material is placed at the intersection between the two tubes, thereby exposing the material to grazing flow on one side and normal incidence sound on the other. This allows the acoustic properties of the material to be evaluated in a no-flow environment, with the effects of grazing flow implicitly included. Although the T-tube method does not directly provide the impedance of the complete liner (the back wall is removed), it does provide a measure of the change in impedance as a result of changing flow conditions. Some of the primary issues with this approach are 1) the limited portion of liner material that can be assessed in an individual measurement, 2) radiation impedance uncertainty, and 3) the inability to study liner resonance behavior as a result of backplate removal.

Received 6 May 2002; accepted for publication 5 September 2003.

*Research Scientist, Structural Acoustics Branch, Aerodynamics, Aerothermodynamics and Acoustics Competency. Member AIAA.

†Senior Research Scientist, Computational Modeling and Simulation Branch, Aerodynamics, Aerothermodynamics and Acoustics Competency. Senior Member AIAA.

‡Research Scientist, Aeroacoustics Branch, Aerodynamics, Aerothermodynamics and Acoustics Competency.

§Senior Research Scientist, Structural Acoustics Branch, Aerodynamics, Aerothermodynamics and Acoustics Competency.

¶SI units of measure and the $e^{i\omega t}$ time convention are used throughout this paper.

A number of modal approaches[5–8] have been conducted in grazing flow impedance tubes, in which the combined effects of grazing flow and acoustics are studied within the same tube. However, with the advent of significantly increased computational and data acquisition capability, finite element approaches[9,10] can now be efficiently utilized. These approaches allow a more realistic study of the combined flow and acoustics effects within a grazing flow tube, and they can be used to educe acoustic liner impedance in multiple-mode and highly reflective environments.

The in situ method requires intrusive measurements. For single-layer liners, this method typically requires two microphones embedded into a representative "patch" of the test liner (additional microphones are required for multiple-layer liners). The transfer function between the complex acoustic pressures measured by these microphones is then used to educe the acoustic impedance. In principle, this method is simple to implement and gives a local, detailed account of the total fluctuating pressures at the measurement microphone locations. In contrast to the modal approaches, this method has the advantage that it does not require a description of the global aeroacoustic field. It is, however, labor-intensive and invasive and is thus subject to installation effects (local damage to the liner by microphone insertion and alteration of surface impedance as a result of the flush-mounted microphone at the liner surface). If liner uniformity is a concern, then this method must be applied at a sufficient number of locations along the liner surface to resolve any potential nonuniformity. Regardless, because of its simplicity, the in situ method remains quite useful,[3] especially if detailed aeroacoustics within the liner are desired.

If the effective uniform surface impedance of a test liner in the presence of grazing flow is desired, then a waveguide method is the only viable choice. Although the actual impedance can vary over the length of the liner because of acoustic nonlinearity, the effective uniform impedance assumption treats the entire liner as having a constant impedance at each location on its surface. This effective uniform impedance ζ_u is given by

$$\zeta_u = \frac{1}{\beta_u}, \qquad \beta_u = \frac{1}{N}\sum_{j=1}^{N}\frac{S_j}{S}\beta_j \tag{1}$$

The segment and total surface areas are S_j and S, respectively. Equation (1) treats the acoustic admittance weighted-averaging process as a lumped-element process adapted from lumped-element parallel electrical circuit theory. This weighted-averaging process assumes that the phase of the sound field incident on the segment of liner over which the averaging is to occur is constant. For frequencies with trace wavelengths at least eight times the length of the liner segment, this weighted averaging has been previously demonstrated to be reasonable.[11]

Waveguide methods provide this effective uniform surface impedance without the need for invasive measurements in the test material. At a minimum, this methodology requires a detailed description of the aeroacoustic environment over a significant portion of the test liner length. For some waveguide methods, such as the finite element method discussed in the current study, the measurement domain is extended beyond the liner to some distance into the hard-wall sections of the flow duct to achieve suitable boundary conditions. In general, significantly more data are needed for waveguide methods than for in situ methods. Depending on the complexity of the chosen implementation, waveguide methods can be used to analyze spatially uniform ($\beta_j = \text{constant}$) or nonuniform ($\beta_j \neq \text{constant}$) surface impedance, sometimes with the same data-acquisition sequence. In addition, although the ability to educe impedance for nonuniform liners exists, the spatial scale of impedance nonuniformity that can be resolved is limited by the spatial resolution of the data-acquisition system. (Data-acquisition requirements increase as the resolution is refined to smaller scales.) Development of an efficient impedance eduction methodology for nonuniform liners is an ongoing research effort and is intended to be the subject of future papers.

There are two purposes of this paper. The first is to assess the accuracy of two waveguide methods for determining the normal incidence acoustic impedance in a grazing incidence tube with no flow. The second is to document progress toward quantifying impedance eduction accuracy for test liners subjected to grazing flows over the Mach-number range of 0.1 to 0.5. The aeroacoustic environment under consideration is assumed to 1) consist of forward and backward-traveling acoustic waves, 2) contain multiple modes, and 3) be acceptably described as having a uniform flow profile. Both methods require a measurement of the complex acoustic pressure profile over the length of the test liner. The single mode method (SMM) is based on the assumption that the sound pressure level and phase decay rates of a single progressive mode can be extracted from this measured acoustic pressure profile. No a priori assumptions regarding the modal content or the amount of modal scattering or reflections are made for the finite element method (FEM). Thus, the FEM can be used to evaluate liners with spatially varying surface impedance.[9] Because propagating modes are scattered and reflected when impedance discontinuities are encountered, the SMM is subject to inaccuracy as a result of intrinsic contamination for liners with spatially varying surface impedance. For this reason, only liners that can be described with a uniform impedance are included in this study. The accuracy of each method (SMM and FEM) is initially established by demonstrating good agreement between impedance values educed in the absence of flow and those educed using normal incidence impedance tube data for two dissimilar types of liners. The relative accuracy of the two methods in the presence of up to Mach 0.5 flow is then assessed by comparing the impedances educed with the FEM to those educed with the SMM.

The remainder of this paper is organized into six sections. The first section contains a discussion of the test objective. The next two sections provide descriptions of the test liners and test facilities used in the current study. The fourth section provides a brief discussion of the theory underlying the two acoustic waveguide methods. The fifth section contains a discussion of the results obtained with the two impedance methodologies using data acquired at NASA Langley Research Center. Key findings are presented in the final section.

Test Objective

The objective of the current test was to acquire a set of data that could be used to evaluate two acoustic waveguide methods, the SMM and the FEM. Because of their similar input data requirements, individual complex acoustic pressure profiles acquired in the NASA Langley Research Center grazing incidence tube (GIT) were used as input for both methods. This ensured that differences between the results from the SMM and FEM were not caused by differences in the measurement process.

For the no-flow case, the normal incidence impedance educed with an acoustic waveguide method in a grazing incidence tube should be identical to the impedance educed in the NASA Langley Research Center normal incidence tube (NIT). Thus, prior to testing in the grazing incidence tube, each liner configuration was first tested in a normal incidence tube. The same liner configuration was then installed into the GIT, and data were acquired at centerline Mach numbers of 0.0, 0.1, 0.3, and 0.5. The $M = 0.0$ data were used to compare each method (SMM and FEM) with the normal incidence tube results, while the $M \geq 0.1$ data were used to draw comparisons between the SMM and FEM.

Previous tests have demonstrated that impedances educed in the normal incidence tube are in excellent agreement with those predicted from first principles (no empiricism). Thus, because normal incidence impedances can be easily educed using the two-microphone method[11,12] in the NIT, this was chosen as the baseline against which the SMM and FEM would be compared in the absence of flow.

Unfortunately, there is no such baseline for the cases with flow. For convenience, the SMM was chosen as a basis for comparison (i.e., the FEM will be compared against the SMM). Clearly, there are differences in the assumptions underlying the SMM and the FEM. Thus, deviations from the SMM should not necessarily be construed as indicative of errors in the FEM. Nevertheless, the selection of a baseline for comparisons is expected to provide increasing value

as additional methods (e.g., improved versions of the FEM) are developed in the future.

Test Liners

Four locally reacting test liners, labeled CT1 (ceramic tubular liner 1), CT2 (ceramic tubular liner 2), CT3 (ceramic tubular liner 3) and PF4 (perforate facesheet liner 4), were carefully chosen to achieve the objectives of the current study. Each liner has an active area (i.e., area exposed to sound in the GIT) of 51 × 408 mm. The salient features of these test liners are described next.

CT1

The CT1 liner (Fig. 1) is the baseline liner for this test. It was fabricated from a uniform-depth portion of ceramic tubular material, which provides a high degree of spatial homogeneity and acoustic linearity, as well as a demonstrated insensitivity to mean flow effects. Perhaps more importantly, the impedance spectrum measured with this liner mounted in the NIT matches the impedance spectrum predicted from first principles.[12] These important features are a result of the small channel diameter (0.8 mm), high channel length-to-diameter ratio (96), high surface porosity (65%), and uniform depth (77 mm). Details of the channel geometry are illustrated in Fig. 1.

CT2

This liner (Fig. 2) is also fabricated with the same ceramic tubular material. For this configuration, however, a stepped-depth variation over a spatial cycle equal to $\frac{1}{8}$th of the total liner length (51 mm) was used. The stepped-depth profile (sometimes titled the "staircase" profile) was designed[11] to maximize normal incidence absorption by targeting nondimensional effective uniform resistance and reactance values of one and zero, respectively, for one spatial cycle. For sufficiently large wavelength-to-spatial cycle ratios, this liner of eight contiguous spatial cycles is presumed to provide a uniform impedance. A sketch of test liner CT2, included in Fig. 2, provides a description of the six steps that comprise one spatial cycle. The axial lengths l_s and depths d_s of these steps are given in Table 1.

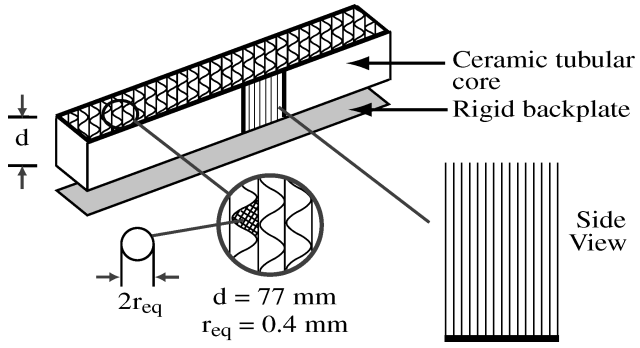

Fig. 1 Sketch of ceramic tubular liner (CT1).

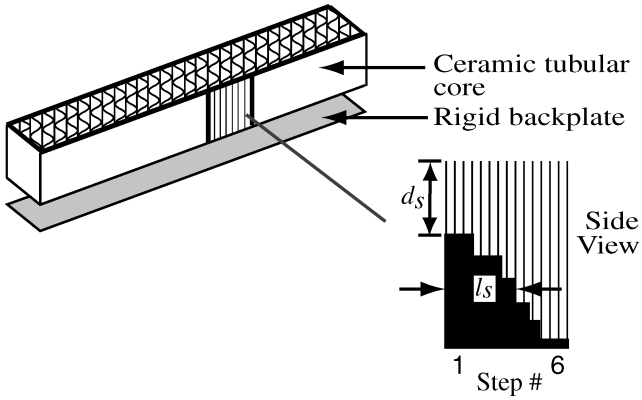

Fig. 2 Sketch of ceramic tubular liner (CT2).

Table 1 CT2 parameters

Step number	l_s, mm	d_s, mm
1	11	31
2	12	40
3	5	50
4	6	59
5	4	69
6	13	77

Table 2 CT3 parameters

Step number(s)	l_s, mm	d_s, mm
1, 13	4	35
2, 12	4	38
3, 11	4	64
4, 10	4	48
5, 9	4	44
6, 8	4	74
7	3	68

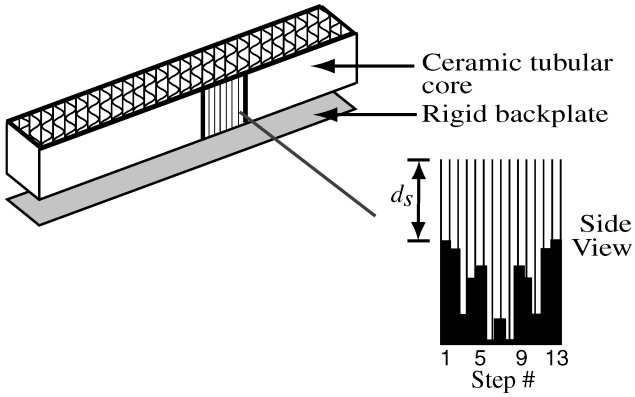

Fig. 3 Sketch of ceramic tubular liner (CT3).

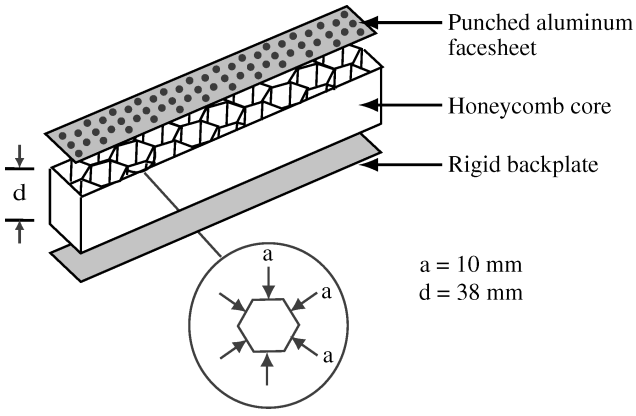

Fig. 4 Sketch of perforate liner (PF4).

CT3

This liner (Fig. 3) is similar to CT2, with the exception that the stepped-depth profile is prescribed in accordance with a quadratic residue sequence.[13] An arrangement of contiguous resonant elements arranged according to this sequence is thought to minimize specular reflection, thereby providing a high level of diffusivity in concert halls. The axial lengths and depths of each 13-step spatial cycle are given in Table 2.

PF4

This conventional, single-layer, perforate liner (Fig. 4) is similar to those currently used for noise suppression in commercial aircraft engines nacelles. It was fabricated from an 0.6-mm-thick aluminum

facesheet with a porosity of 8.7%. This porosity is achieved by a uniform distribution of 0.1-mm-diam holes; thus, the hole length-to-diameter ratio is six. The facesheet is bonded to a hexcell honeycomb with cell depth and equivalent circular diameters of 38 and 10 mm, respectively.

Test Facilities

Two NASA Langley Research Center acoustic waveguides were used extensively for the current study. The first was an NIT, and the other was a GIT. A description of each waveguide and its corresponding test procedure is provided in the following discussion.

Normal Incidence Tube

Description

The NIT is used to determine the normal incidence acoustic impedance of a test material by impinging plane waves onto the surface of the material. This device is a 584-mm-long waveguide with a 51×51 mm cross section. A schematic illustrating this apparatus is shown in Fig. 5. Each test liner was taped such that only a 51-mm-long liner segment was exposed. This liner segment was then carefully clamped to the exit plane of the NIT to avoid sound leakage.

A function generator provides a discrete frequency signal to six 120-W acoustic drivers coupled in parallel. These drivers generate acoustic plane waves at this selected frequency ($0.3 \leq f \leq 3.3$ kHz), with a sound pressure level (SPL) of up to 160 dB at the test liner surface. Acoustic waves that impinge upon the surface of the test liner are reflected to create a standing wave pattern that uniquely characterizes the normal incidence acoustic impedance of the test liner.

Three 6.35-mm-diam ($\frac{1}{4}$-in.) condenser-type microphones are used for data acquisition in the NIT. The first is a reference microphone, which is flush mounted in the top wall of the NIT, 6 mm from the test liner surface. This microphone is used to determine the total SPL at the surface of the test liner. The other two are installed in a rotating plug mounted in the top wall of the NIT. This aluminum plug is designed to allow the microphone positions to be switched in a very convenient and precise manner. The microphones, flush mounted 32 mm apart in the rotating plug, are used to determine the normal incidence impedance of test liners using the switched two-microphone method.[14]

Test Procedure

For the current study, the sound pressure level at the reference microphone location was always set to 120 dB. This level was chosen to minimize nonlinear propagation effects that occur at higher amplitudes and to avoid signal-to-noise limitations associated with lower amplitudes.

Data were acquired for each test liner at frequencies of 0.5, 1.0, 1.5, 2.0, 2.5, and 3.0 kHz. At each test condition, the signals from the two rotating-plug microphones were fed to a fast Fourier transform analyzer to determine the transfer function (magnitude and phase) of the complex acoustic pressures between their two respective locations. The microphone locations were then switched, and a second transfer function was acquired. By applying the switched two-microphone method, the normal incidence impedance was determined.

Grazing Incidence Tube

Description

The Langley GIT, as illustrated in the schematic provided in Fig. 6, enables test liners to be subjected to a controlled aeroacoustic environment in a grazing incidence configuration. The 51-mm-wide $\times$408 mm-long liner is centered lengthwise in the test section, which includes the region from the source plane ($x = 0$ mm) to the exit plane ($x = 816$ mm). The desired aeroacoustic environment in the test section is achieved with the combination of acoustic drivers, a pressurized supply plenum, and a vacuum system. Four 120-W electromagnetic acoustic drivers, whose phase-matched outputs are combined, generate discrete tones from 0.5 to 3.0 kHz with sound pressure levels of up to 155 dB at the liner leading edge. The air supply plenum conditions the flow by means of a specially designed porous-core plenum that allows flow to be combined with the sound field such that sound transmission through the plenum is maximized. Centerline Mach numbers in the test section can range from 0.0 to 0.5. Mach numbers of 0.1 and above are controlled to within ± 0.005.

A 13-mm-wide slot is milled in the top wall to allow a precision-fitted axial traverse bar to transport a 6.35-mm-diam ($\frac{1}{4}$-in.), condenser-type, flush-mounted microphone over the length of the test section. The traversing bar is mechanically driven by a computer-controlled stepper motor to achieve microphone positioning precision to within ± 0.03 mm. Another 6.35-mm-diam reference microphone is flush mounted in the side wall of the GIT, in the same axial plane as the test liner leading edge. This arrangement allows a complete axial mapping of the complex acoustic field throughout the test liner region.

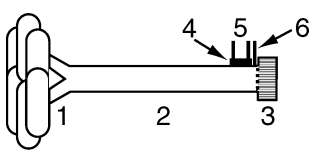

Fig. 5 NASA Langley Research Center NIT: 1, acoustic drivers; 2, waveguide; 3, test liner; 4, rotating plug; 5, measurement microphones; and 6, reference microphone.

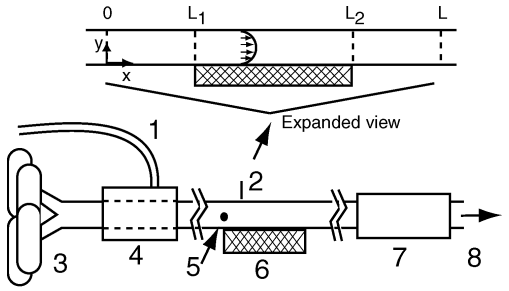

Fig. 6 NASA Langley Research Center GIT: 1, high-pressure air line; 2, traversing microphone; 3, acoustic drivers; 4, plenum with porous core; 5, reference microphone; 6, test liner; 7, termination; and 8, to vacuum pumps.

Test Procedure

For the current study, the sound pressure level at the reference microphone location was always set to 130 dB. This ensured that each waveguide measurement (SMM or FEM) was conducted under equivalent source conditions. These tests were not conducted at 120 dB, as was done with the NIT tests, because of background flow noise concerns. However, 130 dB is still low enough to support linear propagation of the acoustic waves through the waveguide, while also avoiding signal-to-noise limitations associated with lower amplitudes. A signal extraction method[15] was used to acquire the acoustic pressure signals. This method "filters" the microphone output such that the component that is coherent with the discrete tone acoustic source is retained while the remainder of the signal is removed. Usage of this method allows the extraction of quality data even when the signal-to-noise ratio is as poor as -20 dB (SPL of tonal component 20 dB below the SPL of the broadband flow noise measured in the frequency bins just below and above the frequency bin containing the tone of interest). Data were acquired for each test liner at frequencies of 0.5, 1.0, 1.5, 2.0, 2.5, and 3.0 kHz and at centerline Mach numbers of 0.0, 0.1, 0.3, and 0.5. The data-acquisition program automatically positions the traversing microphone at preselected locations x_j from 203 mm upstream of the leading edge to 51 mm downstream of the trailing edge of the liner. At each measurement location, a transfer function is measured between the traversing and reference microphones. This transfer function is used to determine the sound pressure level $\mathrm{SPL}(x_j)$ and phase $\phi(x_j)$ relative to the fixed microphone location. The complex acoustic pressure at a given axial wall location is then determined

from the equation

$$p(x_j, H) = p_{\text{ref}} 10^{\text{SPL}(x_j)/20} e^{i\phi(x_j)} \tag{2}$$

The source-plane acoustic pressure and exit plane impedance are typically functions of y (vertical dimension) and z (spanwise dimension) in these planes. Therefore, y- and z-direction transverse probe microphones should be used to measure these data with the test liner installed. However, the grazing incidence tube used in this study was designed to be operated with source frequencies below the cut-on frequency of higher-order modes, so that only plane waves are supported in the hard-wall sections.

Higher-order modes in the y direction cannot be avoided in the liner region. These higher-order modes, as well as reflections, are generally present in the vicinity of the leading and trailing edges of the specimen. However, because the test liner was installed on only one side of the tube (at $y = 0.0$ mm) higher-order modes in the other (z) direction should only be present at the locations of impedance discontinuity. In addition, the source plane was located 203 mm upstream of the leading edge of the test specimen, and the exit plane was located 203 mm downstream of the trailing edge of the test specimen, each in a hard-wall section of the duct. Because these planes were located four duct diameters away from the liner, higher-order mode effects and reflections from liner edges were not expected to cause appreciable disturbances at either the source or the exit plane. Therefore, the source pressure at each point along the source plane was set to the value measured at the upper-wall source location and the exit impedance at all points in the exit plane were assumed equal. The exit impedance was obtained using the switched two-microphone method[14] with a rotating two-microphone plug installed in the duct side wall near the exit plane. Because the exit impedance is a function of grazing flow Mach number, this measurement was conducted at each test condition.

Acoustic Waveguide Method Theory

Single Mode Method

The SMM uses an infinite waveguide model to educe the impedance of the test liner from the measured complex acoustic wall pressure profile in the x direction for a single, unidirectional propagating mode.[5] As already stated, the maximum frequency tested was 3.0 kHz, which is typically below the cut-on frequency of higher-order hard-wall modes for the flow duct used in this study.

For this method, that portion of the measured complex acoustic pressure profile, which is over the liner (measured on the wall opposite of the liner) but away from the liner leading and trailing edges, is used. For the current study, this distance from the liner edges was typically set at approximately 51 mm or one duct height. Thus, only the measured upper-wall acoustic pressure profile, which was over the central portion (306 mm $\le x \le$ 410 mm) of the liner, was used in the analysis. Figure 7 displays representative SPL and phase (ϕ) data measured along the upper wall of the NASA Langley Grazing Incidence Tube. Contamination of the SPL data near the leading and trailing edges of the liner is clearly evident, which indicates that reflections and/or high-order mode effects are contaminating that portion of the data. The central portion of the data, however, is characterized by a linear SPL and phase decay. This is an indication that a single, progressive mode is dominant over this portion of the liner. If no such linear portion of the data is evident, the SMM cannot be used reliably.

Analytical details of the SMM are provided in detail elsewhere.[5] For convenience, the elements necessary to use the method are repeated here. First, the axial wave number k_x for the dominant progressive mode is computed from the measured portion of the data that has a constant slope using

$$k_x = \frac{\mathrm{d}\phi(x)}{\mathrm{d}x} + \frac{i}{20\log_{10}(e)} \frac{\mathrm{dSPL}(x)}{\mathrm{d}x} \tag{3}$$

In our selected time convention $e^{i\omega t}$, the signs of $\mathrm{dSPL}(x)/\mathrm{d}x$ and $\mathrm{d}\phi(x)/\mathrm{d}x$ are negative for right moving acoustic waves. The dimensionless normal incidence acoustic impedance of the liner can then be determined using

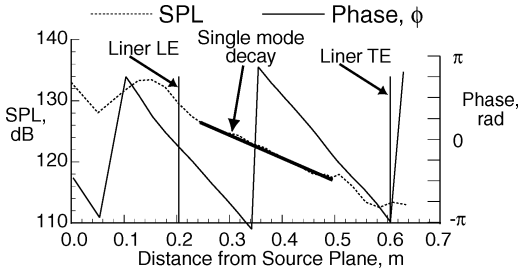

Fig. 7 Sample SPL and phase profiles.

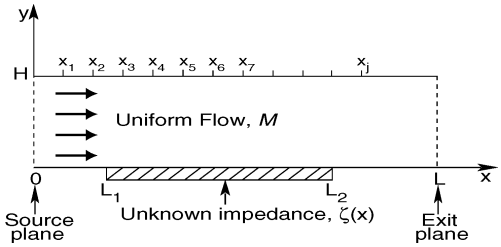

Fig. 8 Geometry and coordinate system for FEM (not to scale).

$$\zeta = -i(k/k_y)[1 - M(k_x/k)]^2 \cot[(kH)(k_y/k)] \tag{4}$$

where

$$\frac{k_y}{k} = \frac{1 - \left[(1 - M^2)(k_x/k) + M\right]^2}{(1 - M^2)} \tag{5}$$

Finite Element Method

Figure 8 depicts the applicable geometry and coordinate system used to model the flow-duct test section for the FEM. This method is described in detail elsewhere,[10] and only sufficient detail is presented here for completeness. The FEM used in this study incorporates the assumptions that the flow profile is uniform and only plane acoustic waves exist in the spanwise z direction. The maximum frequency (3.0 kHz) is below the cut-on frequency for higher-order modes in a hard-wall region for all but the highest Mach number ($M = 0.5$) tested. In the lined section, the two side walls are rigid; thus, the assumption of no higher-order modes in the spanwise direction is reasonable for the frequency range of interest.

The regions upstream ($0 \le x \le L_1$) and downstream ($L_2 \le x \le L$) of the liner contain rigid walls. As described earlier, the complex acoustic pressures are measured at a number of locations along the upper wall (at $x = 0, x_1, x_2, \ldots x_i$) using a microphone flush mounted in the traversing bar.

The FEM finds the solution to the steady-state form of the convected wave equation

$$(1 - M^2)\frac{\partial^2 p}{\partial x^2} + \frac{\partial^2 p}{\partial y^2} - 2ikM\frac{\partial p}{\partial x} + k^2 p = 0 \tag{6}$$

The source-plane acoustic pressure boundary condition is

$$p(0, y) = p_s(y) \tag{7}$$

where $p_s(y)$ is the specified acoustic pressure profile in the transverse y direction at the source plane. Because only plane waves are assumed at this plane, $p_s(y)$ is set to the constant value measured with the axially traversing microphone positioned in the source plane.

The exit-plane boundary condition is

$$\frac{\partial p(L, y)}{\partial x} = \frac{-ikp(L, y)}{M + \zeta_{\text{exit}}} \tag{8}$$

which is derived from the requirement that the exit impedance must equal the ratio of the acoustic pressure to the axial component of acoustic particle velocity in that plane. Because only plane acoustic waves are assumed at the exit plane, ζ_{exit} is taken to be the constant value (for a given frequency and grazing flow Mach number) determined using flush-mounted microphones and plane wave analysis.[14] The boundary condition at each rigid wall is

$$\frac{\partial p}{\partial y} = 0 \tag{9}$$

which indicates that the normal component of acoustic particle velocity vanishes at a rigid wall. Finally, the boundary condition for the lined region of the duct ($L_1 \le x \le L_2$ in Fig. 8) is given by[10]

$$\frac{\partial p(x,0)}{\partial y} = \frac{ikp(x,0)}{\zeta} + 2M\frac{\partial}{\partial x}\left[\frac{p(x,0)}{\zeta}\right] + \frac{M^2}{ik}\frac{\partial^2}{\partial x^2}\left[\frac{p(x,0)}{\zeta}\right] \tag{10}$$

It should perhaps be noted here that the FEM explicitly accounts for exit impedance dependence on the frequency and Mach number, whereas the SMM does not. Instead, the SMM requires that standing waves caused by reflections from the exit plane be sufficiently low as to not impact the "linear decay" portion of the SPL profile over the lined region. Clearly, engineering judgment is required to determine whether an SPL profile is sufficiently linear.

Equations (6–10) constitute a boundary-value problem that can be solved to obtain the upper-wall pressure when the wall impedance is known. The goal of this methodology is to employ the FEM to determine the unknown liner impedance ζ from the measured boundary data by means of an iterative process. The core calculation is to use Eqs. (6–10) to obtain successive sets of upper-wall acoustic pressures, until the computed pressures converge to the measured values to within an acceptable error range. The resulting impedance corresponding to this converged pressure distribution is taken to be the liner impedance.

Results and Discussion

No-Flow Results ($M = 0.0$)

The initial waveguide method comparison was conducted using the uniform-depth CT1 and PF4 liners. These liners were first tested with the NASA Langley Research Center normal incidence impedance tube (NIT).[14] Each liner was then mounted in the grazing incidence tube and tested without flow. Figures 9 and 10 compare the dimensionless liner impedance ($\zeta = \theta + i\chi$) obtained using the three (NIT, SMM, and FEM) methodologies without flow. For the CT1 liner, the SMM and FEM results (depicted with circles and squares, respectively) are well matched to the corresponding NIT results (denoted with + signs). The same comparison holds

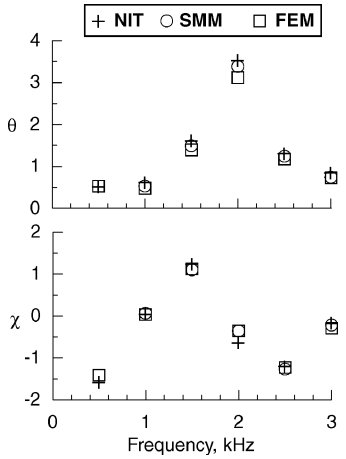

Fig. 9 Ceramic tubular liner (CT1): no flow.

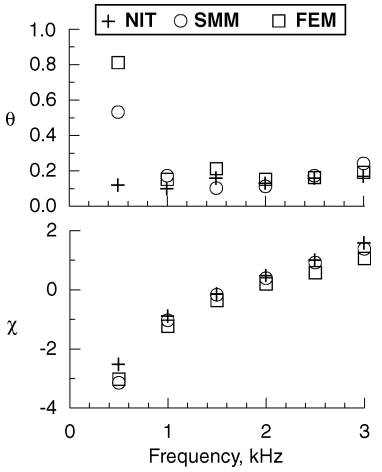

Fig. 10 Perforate liner (PF4): no flow.

for the PF4 liner, except at 0.5 kHz. Although the acoustic reactances χ are still well matched at this frequency, the acoustic resistances θ are significantly different. Possible explanations for this occurrence at 0.5 kHz are provided later in this paper. Similar tests with the CT2 and CT3 liner configurations (not included in this report for the sake of brevity) provided further confirmation that the SMM and FEM educe the correct impedance spectra in the absence of flow.

Previous studies have demonstrated that the acoustic impedance of a ceramic tubular liner, as predicted from first principles,[11] is virtually identical to the impedance educed from measurements in a normal incidence tube. Thus, the impedances educed with the normal incidence impedance tube are taken to be the "baseline" against which the accuracy of results from the two propagation methods will be assessed in the absence of flow. To conduct this assessment, the resistance and reactance error means for the SMM and the FEM were computed using all four liner configurations. For the SMM, the resistance and reactance error means were calculated using

$$\mu_{\theta,\text{SMM}} = \frac{1}{N}\sum_{j=1}^{N} |\theta_{\text{SMM}} - \theta_{\text{NIT}}|_j \tag{11}$$

$$\mu_{\chi,\text{SMM}} = \frac{1}{N}\sum_{j=1}^{N} |\chi_{\text{SMM}} - \chi_{\text{NIT}}|_j \tag{12}$$

where the number of test conditions included in the calculation (N) is 20 (four samples, five test frequencies per sample). Because the SMM could not always be used for the 0.5-kHz impedance data (no linear axial SPL and phase decays evident), only the results for the five frequencies at or above 1.0 kHz are included in these calculations. Similar calculations were performed using the FEM results. For consistency with the SMM results, only the results for frequencies at or above 1.0 kHz were included in these calculations. The results of these error mean calculations are provided here:

$$\mu_{\theta,\text{SMM}} = 0.09, \qquad \mu_{\chi,\text{SMM}} = 0.08$$
$$\mu_{\theta,\text{FEM}} = 0.12, \qquad \mu_{\chi,\text{FEM}} = 0.20 \tag{13}$$

The resistance and reactance error standard deviations for the SMM were calculated from the corresponding variances using

$$\sigma^2_{\theta,\text{SMM}} = \frac{1}{N-1}\sum_{j=1}^{N} (|\theta_{\text{SMM}} - \theta_{\text{NIT}}| - \mu_{\theta,\text{SMM}})^2_j \tag{14}$$

$$\sigma^2_{\chi,\text{SMM}} = \frac{1}{N-1}\sum_{j=1}^{N} (|\chi_{\text{SMM}} - \chi_{\text{NIT}}| - \mu_{\chi,\text{SMM}})^2_j \tag{15}$$

The results of these, and the corresponding FEM results, which were calculated in the same manner, are provided here:

$$\sigma_{\theta,\mathrm{SMM}} = 0.11, \qquad \sigma_{\chi,\mathrm{SMM}} = 0.07$$

$$\sigma_{\theta,\mathrm{FEM}} = 0.14, \qquad \sigma_{\chi,\mathrm{FEM}} = 0.15 \tag{16}$$

These results provide an indication of the dispersion of the resistance and reactance errors about the respective error means. They are approximately the same for each of the methods for the resistance component, although they are not as well matched for the reactance component.

Clearly, values of zero for the error means and standard deviations would indicate an ideal match of waveguide method results to those achieved in the NIT. The deviation from zero for each of these calculations therefore suggests a need for further waveguide method improvements. However, a key difference between the NIT and GIT acoustic conditions can be at least partially to blame for the less-than-perfect comparisons. In the NIT, the sound simultaneously impinges on the entire sample surface with a constant SPL. Conversely, as the sound passes over the length of the liner in the GIT the SPL is typically reduced. Thus, the downstream portions of the liner are not exposed to the same SPLs as the upstream portions. In light of this basic difference between the methodologies, the magnitudes of the error means and standard deviations are considered, for now, to be acceptable.

Flow Results ($M \geq 0.1$)

Next, all four liners (three ceramic and one perforate) were tested in the grazing incidence tube at centerline Mach numbers of 0.1, 0.3, and 0.5. The results are provided in Figs. 11–14. As expected, the acoustic resistance sensitivity to flow velocity is less for the ceramic liners than for the perforate, except at 0.5 kHz. Also, the acoustic resistance is sensitive to flow velocity for the uniform-depth ceramic liner near the antiresonance (2.2 kHz). There were some conditions where the SMM was not applicable because a region of linear decay of SPL and phase could not be extracted from the data. However, when a region of linear decay of SPL and phase could be extracted from the data, SMM and FEM results are typically well matched.

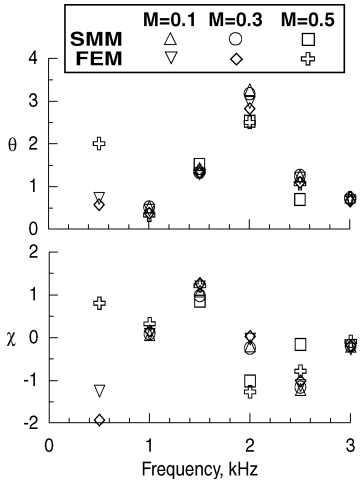

Fig. 11 Ceramic tubular liner (CT1) with flow.

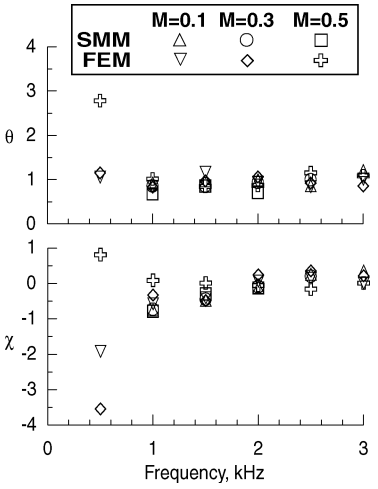

Fig. 12 Ceramic tubular liner (CT2) with flow.

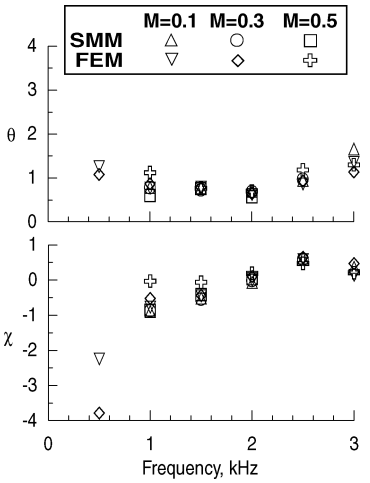

Fig. 13 Ceramic tubular liner (CT3) with flow.

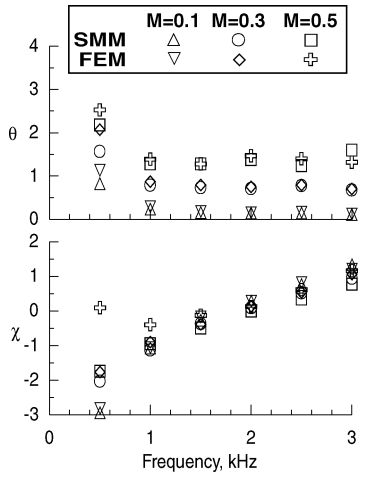

Fig. 14 Perforate liner (PF4) with flow.

Figures 11–13 contain educed impedances for the three ceramic tubular liner configurations. The CT1 (uniform depth) impedance spectrum is typical of a "quarter-wavelength" liner, with a resonance near 1 kHz and an antiresonance near 2 kHz. As expected, the impedance spectra for the CT2 and CT3 liners are relatively constant vs frequency. For all three ceramic tubular liners, the SMM could not be used at 0.5 kHz because linear amplitude and phase decay rates could not be fit to the measured upper-wall acoustic pressure profiles. The FEM also was unstable at 0.5 kHz for these liners, as demonstrated by the significant variability vs flow Mach number. In addition, the resistances for all three ceramic liners are observed to be much less sensitive to flow Mach number (0.5 kHz excluded) than is observed for the perforate liner. In general, the ceramic tubular liners are useful for the evaluation of waveguide methods because the results acquired with a normal incidence impedance tube can be directly compared with those acquired with a flow impedance tube.

Finally, the impedance spectrum for the perforate liner (PF4) is provided in Fig. 14. The acoustic resistance increases uniformly with increasing flow Mach number, while the acoustic reactance is relatively insensitive to changes in flow Mach number. Because of the clear Mach-number dependence of the PF4 acoustic resistance, the ability of the two methods (SMM and FEM) to track one another is especially clear. At frequencies of 1.5 kHz and higher, the acoustic reactance is almost completely a function of the cavity depth and is virtually independent of flow velocity.

There is no "baseline" against which the two acoustic waveguide methods can be compared in the presence of flow. Therefore, one technique for assessing improvements in impedance eduction accuracy is to compare results to determine if the same "answer" can be achieved using each of the two methods. For this purpose, the resistance and reactance error means for the Mach 0.1 data ($\mu_{\theta,M=0.1}$ and $\mu_{\chi,M=0.1}$) were calculated using

$$\mu_{\theta,M=0.1} = \frac{1}{N}\sum_{j=1}^{N} |\theta_{\mathrm{FEM}} - \theta_{\mathrm{SMM}}|_j \tag{17}$$

$$\mu_{\chi,M=0.1} = \frac{1}{N}\sum_{j=1}^{N} |\chi_{\mathrm{FEM}} - \chi_{\mathrm{SMM}}|_j \tag{18}$$

The results for each Mach number included in the current study are provided here:

$$\begin{aligned} \mu_{\theta,M=0.1} &= 0.08, & \mu_{\chi,M=0.1} &= 0.10 \\ \mu_{\theta,M=0.3} &= 0.07, & \mu_{\chi,M=0.3} &= 0.15 \\ \mu_{\theta,M=0.5} &= 0.18, & \mu_{\chi,M=0.5} &= 0.41 \end{aligned} \tag{19}$$

Similarly, the resistance and reactance standard deviations for the Mach 0.1 data ($\sigma_{\theta,M=0.1}$ and $\sigma_{\chi,M=0.1}$) were calculated from the corresponding variances using

$$\sigma^2_{\theta,M=0.1} = \frac{1}{N-1}\sum_{j=1}^{N} (|\theta_{\mathrm{FEM}} - \theta_{\mathrm{SMM}}| - \mu_{\theta,M=0.1})^2_j \tag{20}$$

$$\sigma^2_{\chi,M=0.1} = \frac{1}{N-1}\sum_{j=1}^{N} (|\chi_{\mathrm{FEM}} - \chi_{\mathrm{SMM}}| - \mu_{\chi,M=0.1})^2_j \tag{21}$$

The results for each Mach number included in the current study are provided here:

$$\begin{aligned} \sigma_{\theta,M=0.1} &= 0.08, & \sigma_{\chi,M=0.1} &= 0.09 \\ \sigma_{\theta,M=0.3} &= 0.04, & \sigma_{\chi,M=0.3} &= 0.13 \\ \sigma_{\theta,M=0.5} &= 0.16, & \sigma_{\chi,M=0.5} &= 0.25 \end{aligned} \tag{22}$$

These calculations could only be conducted for test conditions for which both the SMM and the FEM could be exercised. Thus, the number of test points N available for use in each of the preceding calculations varied with Mach number. The values for N were 19, 17, and 13 for the Mach 0.1, 0.3, and 0.5 conditions, respectively.

These error values provide an indication of how well the FEM matches the SMM. However, there is no a priori method to determine which of these is actually closer to the "true" impedance of the test liner. Regardless, as additional methods are evaluated in the same manner, their respective comparisons can be used to demonstrate improvements in impedance eduction methodology.

Data-Processing Issues

It is also important to note the level of complexity involved in the SMM and the FEM. Although the two methods were compared in this study using the same measured data to ensure the quality of the comparison, the SMM does not require the full data set. Specifically, no data outside the lined region are directly used in the SMM analysis procedure. (It was, however, used by the operator to enhance confidence in the data.) Thus, approximately 30% of the data acquired in this study was not needed for the SMM. In addition, the SMM requires significantly less computational time than the FEM.

For the current study, the SMM was exercised using a desktop computer in an interactive manner, in which the operator processed the data for one test condition (one frequency and one Mach number) at a time. This process took approximately 10 s per test condition, of which less than 1 s was used in the actual computation and the remainder was used to visually judge the quality of the data fit. By comparison, the FEM was exercised using a state-of-the-art workstation. This process, which was not interactive, required approximately 60 s of computational time per test condition.

If a large number of conditions are to be analyzed (six frequencies at four Mach numbers gives 24 conditions for the current study, for each liner), the reduced analysis (and data acquisition) time for the SMM can become significant. Thus, when the acoustic pressure magnitude and phase slopes are constant across the length of the liner, the SMM is a good choice. However, for those conditions where the slopes are not constant, the FEM provides a viable alternative.

Discussion of 0.5-kHz Discrepancies

Finally, further studies are planned to better understand why the ceramic tubular liner impedance varies significantly with flow Mach number at 0.5 kHz. Six possible explanations for the discrepancy in the educed impedance (as a function of the flow Mach number) have been suggested to the authors. Each of these explanations is described here (in increasing order of perceived importance), together with a discussion of their relative merits as related to the tests conducted in the current investigation.

1) Flow noise causes a poor signal-to-noise ratio at 0.5 kHz. As indicated in an earlier section, a signal extraction method was used to measure the discrete tone data. For a 1.0-kHz source and the CT1 liner, the SPL of the extracted tone at the trailing edge is much lower than the corresponding trailing edge SPL for 0.5 kHz (i.e., poorer signal-to-noise ratio for 1.0 kHz than for 0.5 kHz). Yet, the 1.0-kHz data do not encounter the same difficulties as observed at 0.5 kHz. Thus, the problems at 0.5 kHz are not believed to be a result of flow-noise issues.

2) Structural vibrations of the GIT are distorting the 0.5-kHz data. To evaluate this concern, four accelerometers were mounted on the GIT, and the acceleration of the walls was measured for each frequency (0.5, 1.0, 1.5, 2.0, 2.5, and 3.0 kHz) at the maximum flow Mach number ($M = 0.5$). Two of the accelerometers were mounted on the side wall of the tube, and two were mounted on the traversing bar. The two pairs of accelerometers (one pair on the side wall, one pair on traversing bar) were mounted approximately 100 mm upstream and 100 mm downstream of the axial center of the lined section. The maximum acceleration measured with any of the accelerometers was 155 μg. This acceleration was measured with an acoustic signal of 135 dB (maximum achievable at this frequency) at 3.0 kHz. The largest acceleration at 0.5 kHz, measured with a sound level of 145 dB, was 10 μg. The impedance eduction process was robust at 3.0 kHz, for which the structural vibration is an order of magnitude greater than is the case for 0.5 kHz. Thus, structural vibrations are not believed to be the cause of the difficulty at 0.5 kHz.

3) The impedance is sensitive to shear-flow effects for highly reflective waves in high-speed flows.[16] The exit-plane reflection factors at 0.5 kHz are 0.04, 0.04, 0.18, and 0.33 at flow Mach numbers of 0.0, 0.1, 0.3, and 0.5, respectively. The corresponding reflection factors at 1.0 kHz, where no discrepancies have been observed, are 0.03, 0.03, 0.07 and 0.35. Clearly, these reflection factors are not significantly different; thus, this hypothesis does not appear to be valid for the impedance tube used in this investigation.

4) The wavelength is too large relative to the length of the liner. The ratio of the acoustic wavelength to liner length is 1.69 for 0.5 kHz. For 1.0 kHz and above, this ratio is 0.84 or less. Thus, because 0.5 kHz is the only test frequency for which this ratio is greater than unity, this hypothesis would appear to have merit. However, the authors have conducted tests with segmented liners[9] that demonstrated the ability of the FEM to educe the impedance of the individual segments correctly. These segments were significantly shorter than the length of the liners included in the current study. If the wavelength-to-liner-length (or in this case, segment length) ratio is critical, the results at higher frequencies would have been expected to have discrepancies. Because this was not the case, this hypothesis also does not appear to be correct. Regardless, future tests will be conducted to confirm this conclusion with uniform impedance liners of variable lengths.

5) Higher-order modes are disturbing the reference microphone response. All of the data used in the SMM and FEM are acquired by taking transfer functions between the traversing and reference microphones. Underlying this data acquisition approach is the assumption that the signal at the reference microphone is constant for the duration of the test (at an individual frequency and Mach number). If this assumption is violated, the results become unreliable. As described in the Test Facilities section, the reference microphone in the side wall of the GIT is located in the same axial plane as the leading edge of the liner. Because higher-order modes are expected to be generated at this impedance discontinuity, the readings at this microphone might be contaminated with these higher-order mode effects. This issue was not initially considered to be of concern because both waveguide methods (SMM and FEM) use the data acquired using the same reference and traversing microphones. However, recall that the SMM only uses that portion of the data that is over the central portion of the liner, whereas the FEM uses additional data extending beyond the leading and trailing edges of the liner into the hard-wall regions. The data over the liner section, which are used in the SMM, are often erratic at 0.5 kHz. This is evidenced by the fact that the SMM could not be exercised at this frequency, indicating that no clear linear acoustic pressure profile could be extracted from the data. Thus, this hypothesis appears to have some merit. As a result of this study, future tests will be conducted with a reference microphone that is in the hard-wall region, away from the impedance discontinuity.

6) This frequency is near an antiresonance. As has been stated earlier, there is always increased difficulty with measurements in the frequency range surrounding antiresonance. For typical locally reacting single-layer liners used in aircraft applications (e.g., the perforated liner used in this study), the acoustic reactance is dominated by $\cot(kd)$. At frequencies near antiresonance, the acoustic reactance approaches $\pm\infty$. At these frequencies, the acoustic resistance also tends to increase significantly. Clearly, this same condition applies as kd approaches zero (i.e., as the frequency approaches zero), as demonstrated in Fig. 10. By comparison, the impedance spectra for the CT2 (staircase geometry) and the CT3 (quadratic-residue geometry) are relatively frequency independent. These configurations were designed to try to achieve dimensionless acoustic resistances and reactances of one and zero, respectively, over the entire frequency range of interest. Clearly, the impedance spectra demonstrate that the design procedures were successful. The difficulty at 0.5 kHz does not appear to be caused by an antiresonance behavior, because these liners were designed such that the acoustic reactance near zero frequency should not become large in magnitude. However, as seen in Figs. 12 and 13, the difficulty at 0.5 kHz persists. Further tests to study this hypothesis are planned in the near future. In addition, future tests will include measurements at frequencies just above and below 0.5 kHz.

In summary, none of these six hypotheses adequately explain the difficulty encountered when the SMM and FEM approaches are used for impedance eduction in the current grazing incidence tube. However, further tests are planned in the near future to more thoroughly explore the last three hypotheses just described.

Conclusions

Based on the results of this work, the following specific conclusions are drawn:

1) In the absence of flow, both waveguide methods included in this study educe impedance spectra that are almost identical with those acquired with a normal incidence impedance tube. Thus, their accuracy for no-flow conditions is high.

2) In the presence of grazing flow, the relative accuracy of impedance eduction is evaluated by comparing the respective results educed with the SMM and the FEM. Whereas the resistance and reactance error means and standard deviations clearly increase with increasing Mach number, their reasonably small values provide confidence that the accuracy of the two waveguide methods is acceptable up to $M = 0.5$.

3) As was expected from their design features, the impedance spectra of the variable-depth (staircase and quadratic-residue) ceramic tubular liners are relatively independent of frequency and flow velocity effects. The uniform-depth ceramic tubular liner is frequency dependent, but is independent of flow velocity effects. This insensitivity to flow velocity makes these liners useful for evaluation of acoustic waveguide methods.

4) When the SMM can be exercised (i.e., linear SPL and phase decay rates can be determined), it provides nearly identical impedances to those educed with the FEM.

5) Because of its relative simplicity and efficiency, the SMM should be used when the propagation data are clearly dominated by a single mode. The FEM is preferred for all other cases.

References

[1]Phillips, B., "Effects of High Wave Amplitude and Mean Flow on a Helmholtz Resonator," NASA TMX-1582, May 1968.

[2]Dean, P. D., "An In Situ Method of Wall Acoustic Impedance Measurement in Flow Ducts," *Journal of Sound and Vibration*, Vol. 34, No. 1, 1974, pp. 97–130.

[3]Malmary, C., Carbonne, S., Auregan, Y., and Pagneux, V., "Acoustic Impedance Measurement with Grazing Flow," AIAA Paper 2001-2193, May 2001.

[4]Feder, E., and Dean, L. W., III, "Analytical and Experimental Studies for Predicting Noise Attenuation in Acoustically Treated Ducts for Turbofan Engines," NASA CR-1373, Sept. 1969.

[5]Armstrong, D. L., "Acoustic Grazing Flow Impedance Using Waveguide Principles," NASA CR-120848, Dec. 1971.

[6]Eversman, W., Nelsen, M. D., Armstrong, D., and Hall, O. J., Jr., "Theoretical and Experimental Analysis of Acoustic Linings for Ducts with Flow," AIAA Paper 71-731, June 1971.

[7]Tester, B. J., "The Propagation and Attenuation of Sound in Lined Ducts Containing Uniform or Plug Flow," *Journal of Sound and Vibration*, Vol. 28, No. 2, 1973, pp. 151–203.

[8]Tester, B. J., "Acoustic Energy Flow in Lined Ducts Containing Uniform or Plug Flow," *Journal of Sound and Vibration*, Vol. 28, No. 2, 1973, pp. 205–215.

[9]Watson, W. R., Tanner, S. E., and Parrott, T. L., "Optimization Method for Educing Variable-Impedance Liner Properties," *AIAA Journal*, Vol. 36, No. 1, 1998, pp. 18–23.

[10]Watson, W. R., Jones, M. G., and Parrott, T. L., "Validation of an Impedance Eduction Method in Flow," *AIAA Journal*, Vol. 37, No. 7, 1999, pp. 818–824.

[11]Parrott, T. L., and Jones, M. G., "Parallel-Element Liner Impedances for Improved Absorption of Broadband Sound in Ducts," *Noise Control Engineering Journal*, Vol. 43, No. 6, 1995, pp. 183–195.

[12]"Standard Test Method for Impedance and Absorption of Acoustical Materials Using a Tube, Two Microphones, and a Digital Frequency Analysis System," *Annual Book of ASTM Standards*, ASTM E1050-98, American Society for Testing and Materials, West Conshohocken, PA, 2000.

[13]Schroeder, M. R., "Binaural Dissimilarity and Optimum Ceilings for Concert Halls: More Lateral Sound Diffusion," *Journal of the Acoustical Society of America*, Vol. 65, No. 4, 1979, pp. 958–963.

[14]Jones, M. G., and Stiede, P. E., "Comparison of Methods for Determining Specific Acoustic Impedance," *Journal of the Acoustical Society of America*, Vol. 101, No. 5, 1997, pp. 2694–2704.

[15]Jones, M. G., "A Comparison of Signal Enhancement Methods for Extracting Tonal Acoustic Signals," NASA TM-1998-208426, May 1998.

[16]Ju, H. B., and Fung, K. Y., "Time-Domain Impedance Boundary Conditions with Mean Flow Effects," AIAA Paper 2000-2003, June 2000.

H. M. Atassi
Associate Editor